# NUMBER FLUCTUATION SPECTROSCOPY OF MOTILE MICROORGANISMS

DALE W. SCHAEFER *and* BRUCE J. BERNE

*From Sandia Laboratories, Albuquerque, New Mexico 87115 and the Department of Chemistry, Columbia University, New York 10027*

ABSTRACT A random-walk model of motility is used to predict the dynamics of fluctuations in the number of particles in a small observation volume. The results show that number fluctuations provide a measure of the mean swimming speed as well as the persistence length. Experimental light-scattering results are presented for three strains of *Escherichia coli* whose motion appears random-walk in nature. For the strain with the longest persistence length, excellent agreement is found with theoretical predictions. For the more erratic strains, however, the shape of the measured scattered light intensity correlation functions indicates the presence of a contribution due to orientational fluctuations.

## INTRODUCTION

Light microscopy of common motile microorganisms indicates that swimming motion is random-walk in nature. That is, a typical microorganism swims in approximately linear segments separated by abrupt changes in direction. Experiments demonstrate that the mean swimming speed $\langle v \rangle$, the mean distance between direction changes $\langle L \rangle$ and the turn angles $\chi$ are affected by parameters such as temperature, metabolite concentration, and light intensity (1–4). Detailed characterization of motility is, therefore, necessary to the understanding of such primitive responses as thermotaxis, chemotaxis, and phototaxis.

In this work we develop a light-scattering method for the characterization of motility. We show theoretically and experimentally that it is possible to measure $\langle v \rangle$ and the persistence length $\langle \Gamma \rangle \equiv \langle L \rangle / [1 - \langle \cos \chi \rangle]$ by analysis of the fluctuations in the number of microorganisms in the focused waist of a laser beam. This is true since the characteristic time $\tau_N$ of number fluctuations is roughly the residence time of a typical particle within the focused waist. This time is a function of $\langle \Gamma \rangle$ and $\langle v \rangle$.

The potential of number fluctuation spectroscopy can be appreciated by consideration of two extremes of particle motion. If $\langle \Gamma \rangle$ is much greater than the mean dimension of the observation or scattering volume $\langle \sigma \rangle$ then $\tau_N \sim \langle \sigma \rangle / \langle v \rangle$. In this free-particle limit, number fluctuation spectroscopy provides a measure of the swimming speed and this method has been exploited to study the thermal response of a smoothly swimming strain of *Escherichia coli* (3). In the opposite extreme ($\langle \Gamma \rangle \ll \langle \sigma \rangle$) a typical particle will execute a many-step random walk within the observation volume. In this

limit the results of Brownian motion theory can be exploited to demonstrate that $\tau_N \propto \langle\sigma\rangle^2/(\langle\nu\rangle\langle\Gamma\rangle)$. Unfortunately, neither the free-particle nor Brownian limit is appropriate to common microorganisms so we concentrate here on the intermediate regime, $\langle\Gamma\rangle \sim \langle\sigma\rangle$.

## THEORY

### *Random Walk Motion*

The dynamics of stochastic phenomena like number fluctuations must be characterized in a statistical manner such as through spectra or correlation functions (5). Because of the very long characteristic time of number fluctuations it is generally convenient to perform experiments in the time domain through measurement of the correlation function of the number of particles in a small observation volume. Theoretical work is, therefore, directed toward calculation of correlation functions. The appropriate spectra can be obtained by Fourier inversion (5).

Although in some cases it is possible to measure number correlation functions by direct microscopic observation, it is generally convenient to obtain the data indirectly through measurement of the correlation function of the scattered light intensity. If the scattering volume is uniformly illuminated, the scattered light intensity $I(\tau)$ at time $\tau$ directly mirrors the number of particles $N(\tau)$ within the scattering volume. The intensity correlation function $\langle I(0)I(\tau)\rangle$ is then directly proportional to the number correlation function (6),

$$\begin{aligned}\langle I(0)I(\tau)\rangle &= \langle I\rangle^2 + \langle \delta I(0)\delta I(\tau)\rangle \\ &\propto \langle N\rangle^2 + \langle \delta N(0)\delta N(\tau)\rangle,\end{aligned} \tag{1}$$

where $[\delta N(\tau) = N(\tau) - \langle N\rangle]$ is this fluctuation in the number of particles within the scattering volume and $\delta I(\tau)$ is the fluctuation in the intensity. The corner brackets denote an ensemble average. If the scattering volume is not uniformly illuminated, Eq. 1 still applies except that $\langle \delta N(0)\delta N(\tau)\rangle$ must reflect the appropriate intensity profile. In fact, Eq. 1 applies if $\langle \delta N(0)\delta N(\tau)\rangle$ is defined as (7)

$$\langle \delta N(0)\delta N(\tau)\rangle \equiv \rho \int d^3\mathbf{r}_1 \int d^3\mathbf{r}_2 \xi^2(\mathbf{r}_1)\xi^2(\mathbf{r}_2)p(\mathbf{r}_2 - \mathbf{r}_1;\tau), \tag{2}$$

where $\rho$ is the number density of scatterers and $\xi(\mathbf{r})$ is the amplitude of the light field scattered by a particle when at position $\mathbf{r}$. $p(\mathbf{r}_2 - \mathbf{r}_1;\tau)$ is the probability distribution for a particle to move from $\mathbf{r}_1$ to $\mathbf{r}_2$ in a time $\tau$. Eq. 2 assumes that the particles are isotropic.

In a typical laser scattering experiment $\xi(\mathbf{r})$ is approximately Gaussian in all three dimensions. If the beam propagates in this $z$ direction and the scattering angle is 90° then

$$\xi(\mathbf{r}) \propto \exp\{[-(x^2 + y^2)/\sigma_1^2] - z^2/\sigma_2^2\}, \tag{3}$$

where $\sigma_1$ and $\sigma_2$ are the points where the intensity profile of the incident beam and the transmission profile of the collection slit are $1/e^2$ of their initial value. The Gaussian profile in the $x$ and $y$ dimensions is expected for the lowest order transverse laser mode and diffraction at the slit produces an approximate Gaussian profile in the $z$ dimension.

All the information on the dynamics of particle motion is contained in the model-dependent distribution $p(\mathbf{r}_2 - \mathbf{r}_1; \tau)$. It is necessary, therefore, to specify this distribution to proceed with the calculation of $\langle \delta N(0) \delta N(\tau) \rangle$. If the displacement $\Delta R = \mathbf{r}_2 - \mathbf{r}_1$ is assumed to be a Gaussian random variable then (8)

$$p(\mathbf{r}_2 - \mathbf{r}_1; \tau) = [\tfrac{2}{3}\pi \langle \Delta R^2(\tau) \rangle]^{-3/2} \exp[- |\mathbf{r}_2 - \mathbf{r}_1|^2 / \tfrac{2}{3} \langle \Delta R^2(\tau) \rangle]. \quad (4)$$

The Gaussian approximation for $p(\mathbf{r}_2 - \mathbf{r}_1; t)$ will be applicable to motile microorganisms in two possible cases. First of all, in the limit discussed above [$\langle \Gamma \rangle \ll \langle \sigma \rangle$], Eq. 4 follows since a many-step random walk yields a Gaussian distribution (7) with $\langle \Delta R^2(\tau) \rangle = \langle v \rangle \langle \Gamma^2 \rangle \tau / \langle \Gamma \rangle$. Eq. 4 is also appropriate if the velocity distribution is Gaussian. Experimental results presented below indicate that this is a reasonable approximation for *E. coli.*

Combining Eqs. 2, 3, and 4, the number term of the intensity correlation function takes the form (7):

$$\langle \delta N(0) \delta N(\tau) \rangle = \langle N \rangle \{\sigma_1^2 / [\sigma_1^2 + \tfrac{2}{3} \langle \Delta R^2(\tau) \rangle]\} \{\sigma_2^2 / [\sigma_2^2 + \tfrac{2}{3} \langle \Delta R^2(\tau) \rangle]\}^{1/2}, \quad (5)$$

where $\langle N \rangle$ is the average number of particles within $\sigma$ ($\langle N \rangle = \pi^{3/2} \sigma_1^2 \sigma_2 \rho$). The problem has, therefore, been reduced to the calculation of the mean-square displacement $\langle \Delta R^2(\tau) \rangle$.

The calculation of $\langle \Delta R^2 \rangle$ requires a detailed model of particle dynamics. To this end we consider a particle to move with constant speed $v$ along a trajectory consisting of straight line segments as indicated in Fig. 1. The average segment length $\langle L \rangle$ is called the mean free path. The angles through which the particle turns are called $\chi$ so that $\mathbf{u}_j \cdot \mathbf{u}_{j+1} = \cos \chi_j$, $\mathbf{u}_j$ being a unit vector in the direction of motion prior to the $j$th turn. Therefore $\langle \cos \chi \rangle$ gives information about correlation in the direction of motion. If $\langle \cos \chi \rangle = 1$, the particle moves in a straight line, whereas if $\langle \cos \chi \rangle = -1$ the particle stays in the region in which it starts. Since the speed is constant, the velocity on the $j$th segment is $\mathbf{v}_j = v\mathbf{u}_j$.

To proceed we make three further assumptions: (*a*) the turns occur at random times so the probability of $n$ turns in time $\tau$ is Poisson distributed:

$$P_n(\tau) = (1/n!) (v\tau / \langle L \rangle)^n \exp(-v\tau / \langle L \rangle); \quad (6)$$

(*b*) the dihedral angle $\alpha_j$ between the planes defined by $(\mathbf{u}_{j-1}, \mathbf{u}_j)$ and $(\mathbf{u}_j, \mathbf{u}_{j+1})$ is randomly distributed so that $\langle \sin \alpha_j \rangle = 0$; (*c*) the turning angles $\chi$ are uncorrelated so that $\langle \cos \chi_i \cos \chi_j \rangle = \langle \cos \chi_i \rangle \langle \cos \chi_j \rangle$ for $i \neq j$.

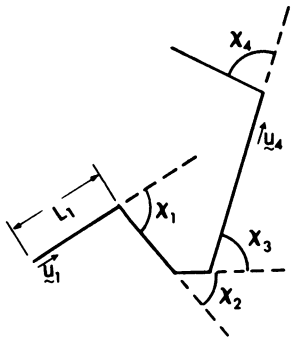


FIGURE 1

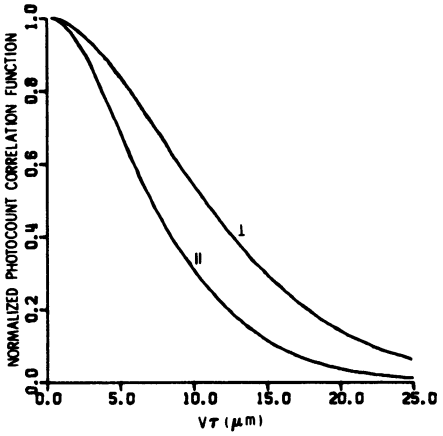


FIGURE 2

FIGURE 1 Typical trajectory of a microorganism with four turning points.

FIGURE 2 Photocount correlation functions of light scattered from systems under uniform translational motion perpendicular and parallel to the incident beam. The translation speeds are $V_{\parallel} = 2{,}765\ \mu m/s$, $V_{\perp} = 5{,}172\ \mu m/s$. Analysis of the curves yields $\sigma_1 = 12.0\ \mu m$, $\sigma_2 = 7.85\ \mu m$.

With the above assumptions it is possible to calculate $\langle \Delta R^2(\tau) \rangle$ by first deriving an expression for the velocity correlation function $\langle \mathbf{v}(0)\mathbf{v}(\tau) \rangle$ and using an exact relation between $\langle \mathbf{v}(0)\mathbf{v}(\tau) \rangle$ and the mean free square displacement,

$$\langle \Delta R^2(\tau) \rangle = 2 \int_0^{\infty} d\tau'(\tau - \tau') \langle \mathbf{v}(0) \cdot \mathbf{v}(\tau') \rangle. \tag{7}$$

The velocity correlation function, however, can be calculated within the assumptions listed above.

$$\langle \mathbf{v}(0) \cdot \mathbf{v}(\tau) \rangle = v^2 \sum_{n=1}^{\infty} P_n(\tau) \langle \mathbf{u}(0) \cdot \mathbf{u}(\tau) \rangle_n, \tag{8}$$

$$= v^2 \exp(-v\tau/\langle \Gamma \rangle), \tag{9}$$

$$\langle \Gamma \rangle \equiv \langle L \rangle / (1 - \langle \cos \chi \rangle), \tag{10}$$

where $\langle\ \rangle_n$ denotes an average after $n$ turns. $\langle \Gamma \rangle$ is the persistence length which equals the mean free path $\langle L \rangle$ if $\chi$ is randomly distributed ($\langle \cos \chi \rangle = 0$). Now $\langle \Delta R^2(\tau) \rangle$ follows from Eqs. 7 and 9:

$$\langle \Delta R^2(\tau) \rangle = 2\langle \Gamma \rangle v\tau - 2\langle \Gamma \rangle^2 [1 - \exp(-v\tau/\langle \Gamma \rangle)]. \tag{11}$$

Eq. 11 is valid for any speed distribution $P(v)$. The original assumption leading to Eq. 5, however, requires that the displacement be a Gaussian random variable, a condidition which is fulfilled for $0 < \tau < \infty$ if the velocity distribution is Gaussian. A

Gaussian velocity distribution, however, follows if the directions are random and the speed distribution has the following form (9),

$$P(v) = (4v^2/\pi^{1/2}v_p^3)\exp(-v^2/v_p^2), \tag{12}$$

where $v_p = \sqrt{\pi}\langle v\rangle/2$ is the most probable speed. Eq. 12 is the Maxwell distribution familiar in the kinetic theory of gases. Although we have neither physical nor physiological justification for application of this distribution to bacteria our results indicate that number fluctuation data can be reasonably interpreted using this distribution. Eq. 11 then, must be averaged over the distribution 12 to give

$$\begin{aligned}\langle \Delta R^2(\tau)\rangle_m = {} & 2\langle\Gamma\rangle\langle v\rangle\tau - 2\langle\Gamma\rangle^2\{1 + [v_p\tau/(\pi^{1/2}\langle\Gamma\rangle)] \\ & - \{1 + [v_p^2\tau^2/(2\langle\Gamma\rangle^2)]\}\{1 - \mathrm{erf}[v_p\tau/(2\langle\Gamma\rangle)]\} \\ & \times \exp[v_p^2\tau^2/(4\langle\Gamma\rangle^2)]\},\end{aligned} \tag{13}$$

where erf is the error function. The subscript $m$ denotes the Maxwellian average. Eq. 13 used in conjunction with Eq. 5 yields the predicted number correlation function as measured by light scattering.

The small and large $\tau$ limits of Eq. 11 correspond to the free particle and Brownian motion cases described in the Introduction. In the small $\tau$ limit

$$\langle \Delta R^2\rangle = \langle v^2\rangle\tau^2; \tau \ll \langle\Gamma\rangle/\langle v\rangle. \tag{14}$$

This limit is applicable whenever $\langle\Gamma\rangle$ is large compared with the linear dimensions of the scattering volume ($\langle\Gamma\rangle \gg \langle\sigma\rangle$). This condition is fulfilled for one of the three strains of *E. coli* studied below. If $\langle\Gamma\rangle$ is short compared with the mean dimension of the scattering volume $\langle\sigma\rangle$ then the large $\tau$ limit of Eq. 11 applies,

$$\langle \Delta R^2\rangle = 2\langle\Gamma\rangle\langle v\rangle\tau; \tau \gg \langle\Gamma\rangle/\langle v\rangle. \tag{15}$$

This is the Brownian limit and the motion appears diffusional in nature with an effective diffusion constant equal to $\langle v\rangle\langle\Gamma\rangle/3$.

If the scattering volume parameters $\sigma$ are known, the predicted number correlation function can be calculated using either Eq. 13, 14, or 15 with Eq. 5.

### *Uniform Motion*

Determination of the scattering volume parameters $\sigma$ is essential to the number fluctuation method. In this section we demonstrate that $\sigma_1$ and $\sigma_2$ in Eq. 5 can be obtained from measured number correlation functions for systems under uniform translational motion. This motion can be achieved by moving the entire sample cell on a translation stage. If the translation speed is much faster than the swimming motion of the scatterers; the distribution $p(\mathbf{r}_2 - \mathbf{r}_1;t)$ in Eq. 2 takes the form

$$p(\mathbf{r}_2 - \mathbf{r}_1;\tau) = \delta[(\mathbf{r}_2 - \mathbf{r}_1) - \mathbf{V}\tau], \tag{16}$$

where V is the translation velocity. Substitution of Eq. 16 into Eq. 2 yields

$$\langle \delta N(0)\delta N(\tau)\rangle = \rho \int \mathbf{dr}\xi^2(\mathbf{r})\xi^2(\mathbf{r} + \mathbf{V}\tau). \tag{17}$$

Thus the number correlation function is proportional to the convolution of the beam profile with itself.

The parameters $\sigma_1$ and $\sigma_2$ can be determined by translating perpendicular and parallel to the incident beam. For example, if V is perpendicular to the incident beam Eqs. 17 and 3 yield

$$\langle \delta N(0)\delta N(\tau)\rangle = \langle N\rangle \exp(-V^2\tau^2/\sigma_1^2). \tag{18}$$

Thus a Gaussian correlation function is predicted whose width is $\sigma_1$. If the sample is translated parallel to the beam the predicted width is $\sigma_2$ rather than $\sigma_1$.

*The Photocount Correlation Function*

Since the experiments reported below are performed using photon correlation methods it is necessary to discuss the relationship between the intensity correlation function (Eq. 1) and the photocount correlation function. The experiment is performed by placing a phototube in the field of the scattered light and measuring the number of photocounts $\mathbf{n}(t)$ detected in a time interval of length $T$ centered at time $t (T \ll \tau_N)$. The photocount correlation function $\langle n(0)n(\tau)\rangle = \langle n(t)n(t + \tau)\rangle_t$ is then constructed by means of a real-time hard-wired computer called a correlator.

The photocount correlation function differs from $\langle I(0)I(\tau)\rangle$ in three respects. First, because of the discrete nature of electrical signals $\langle n(0)n(\tau)\rangle$ contains a shot-noise component at $\tau = 0$. That is, even if the intensity is constant $n(t)$ fluctuates. The $\tau = 0$ point does not appear in the data reported below. In addition to shot noise, dark counts in the detector make an important contribution to $\langle n(0)n(\tau)\rangle$. Since dark counts are random, their effect appears as an additional time-independent contribution $\langle n(0)n(\tau)\rangle$. Finally, a significant amount of light is scattered from the solvent which is not accounted for in Eq. 1. The effect of this background scattering is identical to that of dark counts.

In $n_d$ and $n_b$ are the number of dark and solvent background counts then $\langle n(0)n(\tau)\rangle$ takes the form ($\tau > 0$)

$$\langle n(0)n(\tau)\rangle/\langle n\rangle^2 = 1 + \beta\langle \delta N(0)\delta N(\tau)\rangle, \tag{19}$$

$$\beta = \alpha^2/(\alpha\langle N\rangle + \langle n_d\rangle + \langle n_b\rangle)^2, \tag{20}$$

where $\alpha$ is a constant proportional to the intensity of light scattered by an individual microorganism. Thus the time-dependent part of $\langle n(0)n(t)\rangle$ is proportional to $\langle \delta N(0)\delta N(\tau)\rangle$, but the amplitude of this term is not proportional to $\langle N\rangle^{-1}$ unless $\langle n_d + n_b\rangle \ll \alpha\langle N\rangle$, a condition difficult to achieve in practice.

## EXPERIMENT

The experimental work consists of measurement of the photocount correlation function for light scattered from three strains of *E. coli* (cheC497, AW405, and unc602). Berg and Brown (4) find motility of these strains to be similar to that modeled in Fig. 1. The trajectories appear as relatively straight "runs" separated by short periods of orientation-randomizing "twiddles." The three strains differ primarily in the mean free path $\langle L \rangle$ which Berg and Brown find to vary from 6 $\mu$m for unc602 to 120 $\mu$m for cheC497. The bacterial bodies are approximately 1 $\mu$m in diameter and 2.5 $\mu$m in length.

Experimental apparatus consists of a conventional light-scattering photometer connected to a digital correlator. The incident light from a He-Ne laser (Model 125, Spectra-Physics Inc., Mountain View, Calif.), is attenuated and then focused by a lens on the center of a 1 cm × 1 cm cuvette containing the sample. The lens also serves as the window on a temperature-controlled water bath (±0.05°C). The effective focal length of the lens is 7 cm. The light scattered at 90° is collected through a flat window and focused onto a narrow slit. To minimize coherent effects the photocathode is large enough to encompass many coherence areas of the scattered light field.

After amplification and discrimination the photopulses are correlated by a SAICOR model 42A correlator (SAICOR/Honeywell, Hauppauge, N.Y.). This device was modified by the manufacturer for four-bit digital correlation. Two of the 100 channels are used to measure the total number of photocounts and the total number of sampling intervals. These numbers permit calculation of $\langle n \rangle$ so that the time-independent background $\langle n \rangle^2$ in Eq. 19 can be subtracted.

Samples are grown directly in the scattering cuvettes using modified Hutner's medium (10). We find that the samples are vigorously motile during the late-log and stationary phases of the growth cycle. We estimate that $0.1 < \langle N \rangle < 1$ for all the samples studied here.

The sample cell is mounted directly on a translation stage to permit measurement of $\sigma_1$ and $\sigma_2$ as discussed above. The bacterial sample itself is used to measure $\sigma_1$ by translating the sample perpendicular to the incident laser beam. $\sigma_2$ is measured by replacing the sample with a 1 cm × 4 cm × 4 cm cuvette containing a dilute solution of 1 $\mu$m-diam polystyrene spheres and translating the cell parallel to the beam. Fig. 2 shows the measured photocount correlation function for both translation directions. The time-independent background has been subtracted. Since the curves show slight deviation from the Gaussian shape, the parameters $\sigma$ are extracted from the initial decay of the correlation functions. The values of $\sigma$ obtained from Fig. 2 are used in the analysis of the strain unc602 although translation data for other samples is very similar.

## RESULTS AND DISCUSSION

The measured photocount correlation functions for all three strains are displayed in Fig. 3. The time-independent background has been removed and the data are normal-

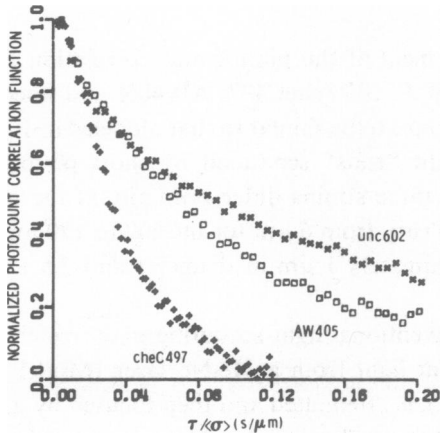


FIGURE 3

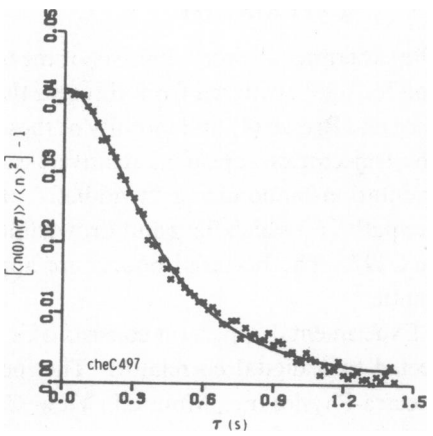


FIGURE 4

FIGURE 3 Measured photocount correlation functions for *E. coli* strains cheC497, AW405, and unc602. The time-independent background is removed and the data are normalized by dividing the ordinate of each point by the ordinate of the first point. Data were taken at 30.8°C.

FIGURE 4 Measured photocount correlation function for *E. coli* cheC497. Solid line represents a least-squares minimization using Eqs. 5, 14, and 19. Solid line is plotted with $\langle v^2 \rangle^{1/2} = 26.9$ $\mu$m/s. The scattering volume parameters are $\sigma_1 = 13.75$ $\mu$m, $\sigma_2 = 7.81$ $\mu$m.

ized by dividing each ordinate by the ordinate of the first point. The data are plotted versus $\tau/\langle\sigma\rangle$ since the scattering volume is not identical for each sample.

The striking difference in decay times of the curves in Fig. 3 is consistent with the patterns of motility observed under a microscope. The short correlation time for cheC497 indicates that the persistence length of this strain is much longer than the mean dimension of the scattering volume. The much longer decay time of the curves for AW405 and unc602 is indicative of slower swimming speeds and shorter persistence lengths.

The data for cheC497 are most easily analyzed since this strain behaves as a free particle over distances of the order of $\langle\sigma\rangle$. The cheC497 data are analyzed, therefore, using Eqs. 5, 14, and 19. A two-parameter ($\beta$ and $\langle v^2 \rangle$) least-square minimization leads to the theoretical curve plotted in Fig. 4. The value $\langle v^2 \rangle^{1/2}$ for the best fit is consistent with the tracking data on this strain (4). The fact that the theoretical curve falls within the scatter over most of the curve indicates that the Maxwellian speed distribution assumed in the derivation of Eq. 5 is reasonable. It should be pointed out, however, that measured correlation functions are very insensitive to higher moments of the speed distribution.

For strains AW405 and unc602, data analysis is hampered by the fact that three parameters are required ($\beta$, $\langle v \rangle$ and $\langle \Gamma \rangle$) and by the fact that the initial decay of the measured curves does not follow the $\tau^2$ behavior predicted by Eq. 5. The three-parameter problem increases the confidence limits on the measured parameters,

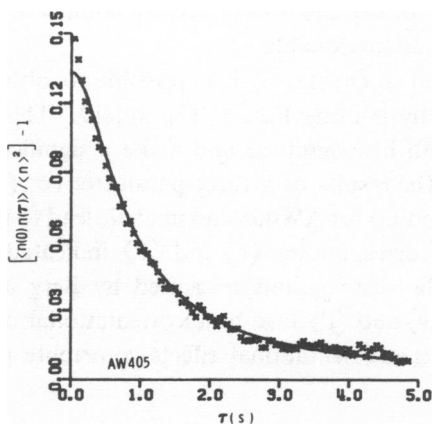


FIGURE 5

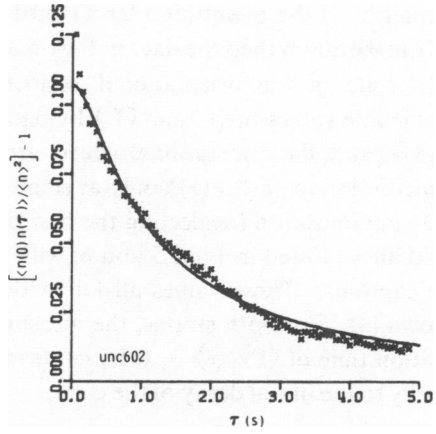


FIGURE 6

FIGURE 5 Measured photocount correlation function for *E. coli* AW405. Solid line represents a least-squares minimization using Eqs. 5, 13, and 19. Solid line is plotted with the parameters $\langle v \rangle = 13.5\ \mu m/s$ and $\langle \Gamma \rangle = 8.0\ \mu m$. The measured scattering volume parameters are $\sigma_1 = 12.5$, $\sigma_2 = 7.81$.

FIGURE 6 Measured photocurrent correlation function for *E. coli* unc602. Solid line represents a least-squares minimization using Eqs. 5, 13, and 19. Solid line is plotted with $\langle v \rangle = 13.2\ \mu m/s$ and $\langle \Gamma \rangle = 3.9\ \mu m$. The measured scattering volume parameters are $\sigma_1 = 12.0\ \mu m$, $\sigma_2 = 7.85\ \mu m$.

whereas the initial linear decay of the correlation function indicates that the assumptions leading to Eq. 5 are not fulfilled for small $\tau$.

We believe the most reasonable explanation of the linear initial decay observed in Figs. 5 and 6 is that there is an additional fluctuating component in the scattered light intensity due to orientation fluctuations. That is, since scatterers are not spherical, the amplitude of the scattered light field will be modulated as the axis of the particle changes with respect to the polarization of the incident light and the scattering plane.

Microscopic observation suggests two types of orientational motion: corkscrew rotation as well as changes in swimming direction. The fact that the linear decay is not observed for the cheC497 indicates that it is the latter type of motion which leads to the observed linear decay.

Orientation fluctuations would lead to an additional contribution to $\langle I(0)I(\tau) \rangle$ whose characteristic time is the time required for randomization of the swimming direction. In particular, if $A(\tau)$ is an orientation-dependent amplitude factor then $I(\tau) = A(\tau)N(\tau)$ for uniform illumination. If $A(\tau)$ and $N(\tau)$ are independent Eq. 1 becomes

$$\langle I(0)I(\tau) \rangle = \langle A \rangle^2 \langle N \rangle^2 + \langle A \rangle^2 \langle \delta N(0) \delta N(\tau) \rangle + \langle N \rangle^2 \langle \delta A(0) \delta A(\tau) \rangle. \quad (21)$$

Thus $\langle I(0)I(\tau) \rangle$ appears as the superposition of a background, number and orienta-

tion term. If the orientation term (third term of Eq. 21) decays rapidly compared to the number term then the data in Figs. 5 and 6 are reasonable.

In spite of the orientational contribution to $\langle n(0)n(\tau)\rangle$ it is possible to obtain reasonable values of $\langle v\rangle$ and $\langle\Gamma\rangle$ by data analysis using Eqs. 5, 13, and 19. This is true because the orientational effects are small in magnitude and make a significant contribution to $\langle n(0)n(\tau)\rangle$ only at small $\tau$. The results of a three-parameter ($\beta$, $\langle v\rangle$, $\langle\Gamma\rangle$) minimization (neglecting the first data point) for AW405 and unc602, lead to the solid lines plotted in Figs. 5 and 6, with the corresponding $\langle v\rangle$ and $\langle\Gamma\rangle$ indicated in the captions. These values all fall within the distributions measured by Berg and Brown (4). For both strains, the measured $\langle v\rangle$ and $\langle\Gamma\rangle$ lead to an orientational correlation time of $\langle\Gamma\rangle/\langle v\rangle \sim 0.5$s, confirming that orientational effects contribute primarily to the initial decay of the curve.

## CONCLUSION

We have developed a general theoretical model of the dynamics of number fluctuations. The predictions of this theory were tested using three strains of *E. coli* with different persistence lengths. The results indicate that (*a*) the Gaussian velocity distribution is a reasonable approximation for the interpretation of *E. coli* data; (*b*) that reasonable values of the swimming speed and persistence length can be extracted from number fluctuation data; and (*c*) that orientational contributions to the initial decay of $\langle n(0)n(\tau)\rangle$ are observed due to the aspheric shape of the scatterers.

This work supported by the U.S. Energy Research and Development Administration and by the National Science Foundation.

*Received for publication 3 March 1975.*

## REFERENCES

1. ADLER, J. 1969. Chemoreceptors in bacteria. *Science (Wash. D.C.).* **166**:1588.
2. CLAYTON, R. K. 1964. Phototaxis in microorganisms. *In* Photophysiology, Vol. VII. 51.
3. BANKS, G., D. W. SCHAEFER, and S. S. ALPERT. 1975. Light-scattering study of the temperature dependence of *Escherichia coli* motility. *Biophys. J.* **15**:253.
4. BERG, H. C., and D. A. BROWN. 1972. Chemotaxis in *Escherichia coli* analyzed by three-dimensional tracking. *Nature (Lond.).* **239**:500.
5. Davenport, W. B., and W. L. ROOT. 1958. Random Signals and Noise. McGraw-Hill, Inc., New York.
6. SCHAEFER, D. W., and B. J. BERNE. 1972. Light scattering from non-Gaussian concentration fluctuations. *Phys. Rev. Lett.* **28**:475.
7. SCHAEFER, D. W. 1973. Dynamics of number fluctuations: motile microorganisms. *Science (Wash. D.C.).* **180**:1293.
8. CHANDRASEKHAR, S. 1943. Stochastic problems in physics and astronomy. *Rev. Mod. Phys.* **15**:1.
9. DANIELS, F., and R. A. ALBERTY. 1961. Physical chemistry. Chap. 11. John Wiley & Sons, Inc., New York.
10. COHEN-BACIRE, G., W. R. SISTROM, and R. Y. STANIER. 1957. Kinetic studies of pigment synthesis by non-sulfur purple bacteria. *J. Cell. Comp. Phys.* **49**:25.